

## A theoretical Taylor–Galerkin model for first-order hyperbolic equation

Tony W. H. Sheu<sup>\*,†,‡</sup> and P. H. Lee<sup>§</sup>

*Department of Engineering Science and Ocean Engineering, National Taiwan University,  
73 Chou-Shan Rd., Taipei, Taiwan, R.O.C.*

### SUMMARY

This paper presents a class of Taylor–Galerkin (TG) finite-element models for solving the first-order hyperbolic equation which admits discontinuities. Five parameters are introduced for purposes of controlling stability, monotonicity and accuracy. In this paper, the total variation diminishing concept and the theory of  $M$ -matrix are applied to construct a monotonic TG model for capturing discontinuities. To avoid making the scheme overly diffusive, we apply a flux-corrected transport (FCT) technique of Boris and Book to overcome the difficulty with anti-diffusive flux. In smooth flow regions, our strategy of developing the temporal and spatial high-order TG finite-element model is based on modified equation analysis. In regions where discontinuity is encountered, we resort to two dispersively more accurate models to make the prediction accuracy as high as that obtained in smooth cases. These models are developed using the entropy-increasing principle and the theory of group velocity. Guided by this theory, a slower group velocity should be used ahead of the shock. To avoid a train of post-shocks, free parameters should be chosen properly to obtain a group velocity which takes on a larger value than the exact phase velocity. In this paper, we also apply the entropy-increasing principle to determine free parameters introduced in the finite-element model. Under the entropy-increasing requirement, it is mandatory that coefficients of the even and odd derivative terms shown in the modified equation should change signs alternatively in order to avoid non-physical wiggles. Several benchmark problems have been investigated to confirm the integrity of these proposed characteristic models. Copyright © 2003 John Wiley & Sons, Ltd.

**KEY WORDS:** Taylor–Galerkin; discontinuities; monotonicity;  $M$ -matrix; theory of group velocity; entropy-increasing principle

---

\*Correspondence to: Tony W. H. Sheu, Department of Engineering Science and Ocean Engineering, National Taiwan University, 73 Chou-Shan Rd., Taipei, Taiwan, R.O.C.

†E-mail: twhsheu@ntu.edu.tw

‡Professor.

§Graduate student.

Contract/grant sponsor: National Science Council of the Republic of China; contract/grant number: NSC 88-2611-E-002-025

## 1. INTRODUCTION

Study of pure advection equation is considered as an essential step towards suppressing convective instabilities for problems in areas of gas dynamics, shallow-water hydraulics and aeroacoustics. This explains why development of numerical models for first-order hyperbolic equations has occupied the centre stage of computational fluid dynamics in the past few decades [1]. In the finite-element context, several upwind variants capable of preventing convective instability have been proposed in the literature. Methods that are often referred to include the characteristic finite-element method [2], discontinuous finite-element method [3], and characteristic-Galerkin finite-element method [4]. Another class of Petrov–Galerkin methods [5, 6] has also gained widespread acceptance. The main difference being the methodology of introducing the upwind mechanism into the variational statement. In this study, the hyperbolic solver will be developed within the Taylor–Galerkin (TG) framework [7], which has been applied with great success in many practical applications [8, 9].

When a numerical method is applied to solve a non-dispersive wave equation, the discretization error will make its modified equation dispersive. The direct result is that the numerical speed of propagation (or phase velocity) will be a function of wave number [10]. The prediction quality, thus, depends highly on the discrete dispersion relation. For this reason, knowledge of group velocity is essential in the hyperbolic finite-element development [11, 12]. By exploiting group velocity theory, we will develop a dispersively more accurate finite-element model in this paper.

One can exploit another guideline to minimize the dispersion error. In physical terms, entropy is not allowed to decrease when a wave propagates. By employing the entropy-increasing principle [13], we are led to control dispersive errors and avoid continuous growth of the solution due to anti-dissipative errors by assigning the correct signs of leading even and odd derivative terms.

The remainder of this paper is organized as follows. Section 2 presents the essential features of the five-parameter TG finite-element model. This is followed by the construction of TG finite-element models. In Section 4, free parameters used in the low-order TG finite-element model are determined using the total variation diminishing concept and the theory of  $M$ -matrices. In Section 5, a high-order finite-element model is developed by virtue of modified equation analysis, entropy-increasing principle, and the theory of group velocity. We then present validation results in Section 6. Finally, we draw conclusions in Section 7.

## 2. SOME FUNDAMENTALS

We consider in this paper the following model equation:

$$\frac{\partial u}{\partial t} + \frac{\partial f}{\partial x} = 0 \quad (1)$$

Note that  $c$  in the physical flux term  $f(u) = cu$  is a positive constant. Subject to  $u(x, t = 0) = \exp(ikx)$ , the analytic solution  $u_{\text{exact}}(x, t)$  for (1) can be expressed in terms of the phase function  $S(\equiv kx - \omega t)$ :

$$u_{\text{exact}}(x, t) = \exp[i(kx - \omega t)] \quad (2)$$

In the above,  $k$  and  $\omega$  denote the wave number and the frequency, respectively.

The phase speed is, by definition, the speed of phase line advancing normally to itself. As a result,  $\nabla S (\equiv \partial S / \partial x) = k$  and  $\partial S / \partial t = -\omega$ . Along a phase line  $S(x, t) = \text{constant} (\equiv S_0)$ , we have  $dS = \partial S / \partial t dt + \nabla S dx = 0$ , and, in turn, the phase speed  $c = \omega / k$ . As a result, the analytic dispersion relation for (1) is

$$\omega = \omega(k) = ck \quad (3)$$

In the light of the above dispersion relation, the phase speed is known to be independent of  $k$ . The hyperbolic equation to be investigated is, therefore, a non-dispersive differential equation.

Like other numerical methods, finite-element approximation of (1) may introduce dissipation and dispersion errors. To account for both types of errors, we can represent the numerical solution as follows:

$$u(x_j, t) = \exp\left(-c \frac{k_r}{\Delta x} t\right) \exp\left[ik \left(x_j - \frac{k_i}{k\Delta x} ct\right)\right] \quad (4)$$

Here,  $k_r$  and  $k_i$  signify the amounts of dissipation and dispersion errors, respectively. The consistency property [14] requires that  $k_r/\Delta x$  approach zero while  $k_i/\bar{\alpha}$  approach 1, where  $\bar{\alpha} = k\Delta x$  is known as the modified wave number.

### 3. TAYLOR–GALERKIN FINITE-ELEMENT MODEL WITH CONSISTENCY AND STABILITY PROPERTIES

Our approximation of Equation (1) starts with

$$\sum_{el=1}^{n_{el}} \int_{\Omega^{el}} \int_{t_n}^{t_{n+1}} W(x) \left( \frac{\partial u}{\partial t} + \frac{\partial f}{\partial x} \right) dt d\Omega^{el} = 0 \quad (5)$$

Here, the weighting function  $W(x)$  has the same form as the shape function for  $u$ . In this study, we choose the TG finite-element model due to its applicability to multi-dimensional analyses. As the name implies, TG model development involves expanding  $f$  with respect to time  $t$  in Taylor series. In this study, the expansion is terminated at the third-order accuracy. Inspired by the work of Baker and Kim [15], we introduce five parameters  $\alpha$ ,  $\beta$ ,  $\gamma$ ,  $\mu$ ,  $\omega$  to approximate  $f$  for purposes of controlling dissipation and dispersion errors.

$$\begin{aligned} f &= f^n + c \left( \alpha \frac{\partial u}{\partial t} - \beta \frac{\partial f}{\partial x} \right)^n (t - t_n) \\ &+ \frac{1}{2} c^2 \left( \omega \frac{\partial^2 f}{\partial t^2} + \gamma \frac{\partial^2 u}{\partial t \partial x} - \mu \frac{\partial^2 f}{\partial x^2} \right)^n (t - t_n)^2 + O((t - t_n)^3) \end{aligned} \quad (6)$$

Note that the introduced free parameters in Equation (6) are constrained by  $\alpha + \beta = 1$  and  $\gamma + \mu + \omega = 1$ .

The derivation is followed by substituting

$$u_t^n = \frac{1}{\Delta t} (u^{n+1} - u^n) - \frac{c^2 \Delta t}{2} u_{xx}^n \quad (7a)$$

$$u_{tt}^n = \frac{2}{\Delta t^2} (u^{n+1} - u^n) + \frac{2c}{\Delta t} u_x^n \quad (7b)$$

into (6) to render the following ordinary differential equation:

$$\begin{aligned} f = f^n + c \left( \alpha \left( \frac{1}{\Delta t} (u^{n+1} - u^n) - \frac{c^2 \Delta t}{2} u_{xx}^n \right) - \beta \frac{\partial f}{\partial x} \right)^n (t - t_n) \\ + \frac{1}{2} c^2 \left( \omega \left( \frac{2}{\Delta t^2} (u^{n+1} - u^n) + \frac{2c}{\Delta t} u_x^n \right) \right. \\ \left. + \gamma \frac{\partial u}{\partial x} \left( \frac{1}{\Delta t} (u^{n+1} - u^n) - \frac{c^2 \Delta t}{2} u_{xx}^n \right) - \mu \frac{\partial^2 f}{\partial x^2} \right)^n (t - t_n)^2 + O((t - t_n)^3) \end{aligned} \quad (8)$$

In this paper, we consider the linear element. As a result,  $\mu$  in Equation (6) plays no role and is, thus, not considered. The resulting TG representation of (1) can be rewritten in terms of the Courant number  $v(\equiv \Delta t/\Delta x)$  and the free parameters:

$$\begin{aligned} \frac{1}{2} \left( \frac{1-\omega}{3} + \left( 1 - \alpha - \omega + \frac{\gamma}{2} \right) v + \gamma v^2 \right) u_{j+1}^{n+1} + \left( \frac{2(1-\omega)}{3} - \gamma v^2 \right) u_j^{n+1} \\ + \frac{1}{2} \left( \frac{1-\omega}{3} + \left( -1 + \alpha + \omega - \frac{\gamma}{2} \right) v + \gamma v^2 \right) u_{j-1}^{n+1} \\ = \left( \frac{1-\omega}{6} + \frac{(-\alpha + \gamma/2)v}{2} + v^2 \left( \frac{1}{2} + \frac{\omega}{2} - \beta \right) \right) u_{j+1}^n \\ + 2 \left( \frac{(1-\omega)}{3} - v^2 \left( \frac{1}{2} + \frac{\omega}{2} - \beta \right) \right) u_j^n \\ + \left( \frac{1-\omega}{6} + \frac{(\alpha - \gamma/2)v}{2} + v^2 \left( \frac{1}{2} + \frac{\omega}{2} - \beta \right) \right) u_{j-1}^n \end{aligned} \quad (9)$$

Define  $\Delta^+ u_j^n = u_{j+1}^n - u_j^n$  and  $\Delta^- u_j^n = u_j^n - u_{j-1}^n$ , Equation (9) can be further written in the  $\delta$ -form as

$$u_j^{n+1} - \tilde{C}_{j+1/2} \Delta^+ u_j^{n+1} + \tilde{C}_{j-1/2} \Delta^- u_j^{n+1} = u_j^n + C_{j+1/2} \Delta^+ u_j^n - C_{j-1/2} \Delta^- u_j^n \quad (10)$$

where

$$\tilde{C}_{j+1/2} = -\frac{1}{6} - \frac{(1 - \alpha - \omega + \gamma/2)v}{2(1 - \omega)} - \frac{\gamma v^2}{2(1 - \omega)} \quad (11a)$$

$$\tilde{C}_{j-1/2} = -\frac{1}{6} - \frac{(-1 + \alpha + \omega - \gamma/2)v}{2(1 - \omega)} - \frac{\gamma v^2}{2(1 - \omega)} \tag{11b}$$

$$C_{j+1/2} = \frac{1}{6} + \frac{(-\alpha + \gamma/2)v}{2(1 - \omega)} + \frac{v^2(\frac{1}{2} + \omega/2 - \beta)}{1 - \omega} \tag{11c}$$

$$C_{j-1/2} = \frac{1}{6} + \frac{(\alpha - \gamma/2)v}{2(1 - \omega)} + \frac{v^2(\frac{1}{2} + \omega/2 - \beta)}{1 - \omega} \tag{11d}$$

We conduct first the modified equation analysis of second kind by performing Taylor series expansion on each term in Equation (9). After some algebra, we can obtain the following modified equation for the model equation (1):

$$u_t + cu_x = \tau_2 u_{xx} + \tau_3 u_{xxx} + \tau_4 u_{xxxx} + \dots \tag{12}$$

where

$$\begin{aligned} \tau_2 &= \frac{\Delta x^2 v^2 (-1 + \alpha + \beta)}{\Delta t (-1 + \omega)} \\ \tau_3 &= \frac{-\Delta x^3 v^3}{12 \Delta t (-1 + \omega)^2} \\ &\quad (4 - 12\alpha + 12\alpha^2 + 12\alpha\beta - 8\omega + 4\omega^2 - 12\alpha\gamma - 6\beta\gamma + 6\omega\gamma + 3\gamma^2) \\ \tau_4 &= \frac{\Delta x^4 v^2}{24 \Delta t (-1 + \omega)^3} \\ &\quad (-2\beta + 2\omega + 4\beta\omega - 4\omega^2 - 2\beta\omega^2 + 2\omega^3 - 6v^2 + 24\alpha v^2 - 36\alpha^2 v^2 \\ &\quad + 24\alpha^3 v^2 + 24\alpha^2 \beta v^2 + 12\beta^2 v^2 + 18\omega v^2 - 48\alpha\omega v^2 + 12\alpha^2 \omega v^2 \\ &\quad - 24\beta\omega v^2 - 12\beta^2 \omega v^2 - 6\omega^2 v^2 + 24\alpha\omega^2 v^2 + 24\beta\omega^2 v^2 - 6\omega^3 v^2 \\ &\quad + 12\alpha\gamma v^2 - 36\alpha^2 \gamma v^2 - 12\beta\gamma v^2 - 24\alpha\beta\gamma v^2 + 12\omega\gamma v^2 + 12\alpha\omega\gamma v^2 \\ &\quad + 12\beta\omega\gamma v^2 - 12\omega^2 \gamma v^2 + 3\gamma^2 v^2 + 18\alpha\gamma^2 v^2 + 6\beta\gamma^2 v^2 - 9\omega\gamma^2 v^2 - 3\gamma^3 v^2) \end{aligned}$$

Thanks to the above modified equation, the proposed finite-element model is confirmed to accommodate the consistency property [16] since discretization errors diminish as  $\Delta x$  approaches zero.

We then conduct the Fourier (or von Neumann) stability analysis. The amplification factor for the present TG model is shown to have the following form:

$$G = \frac{\mathbf{a} + \mathbf{b}i}{\mathbf{c} + \mathbf{d}i} \tag{13}$$

where

$$\mathbf{a} = 2((2 - 2\omega + 3(2\beta - 1 - \omega)v^2) + (1 - \omega - 3(2\beta - 1 - \omega)v^2) \cos(\beta))$$

$$\mathbf{b} = -3(2\alpha - \gamma)v \sin(\beta)$$

$$\mathbf{c} = 4 - 4\omega - 6\gamma v^2 + (2 - 2\omega + 6\gamma v^2) \cos(\beta)$$

$$\mathbf{d} = -3(-2 + 2\alpha + 2\omega - \gamma)v \sin(\beta)$$

Note that  $|G| \leq 1$  for all chosen parameters and the scheme is unconditionally stable. The exhibited consistency and stability properties ensure that convergent TG solutions can be obtained irrespective of the chosen free parameters [17].

It now remains to decide what values of the free parameters are desirable for obtaining low- and high-order TG solutions. These two solutions are necessary to obtain the flux corrected transport (FCT) finite-element solution. The  $M$ -matrix and total variation diminishing theories for the monotonic model and the modified equation analysis, group velocity theory and entropy increasing principle for the less dispersive model will be used to achieve different goals.

#### 4. MONOTONIC SOLUTIONS

Within the FCT framework, the key to successful development of the TG finite-element model lies in applying a dispersively more accurate model in the smooth flow regime and a monotonic model in the flow where discontinuities may develop. Pursuit of high accuracy is another important task to make the discontinuity-capturing model robust.

##### 4.1. Total variation diminishing model

According to Lax [15], the total variation of a physically possible solution  $u(x, t)$  to the linear hyperbolic equation (1) is defined as  $\text{TV} = \int |\partial u / \partial x| dx$ . For suppressing oscillations in the vicinity of discontinuities,  $\text{TV}(u)$  is not allowed to increase with time. One way to achieve this goal is to employ a total variation diminishing (TVD) discrete model. We say that a discrete model is total variation diminishing in time if

$$\text{TV}(u^{n+1}) \leq \text{TV}(u^n) \quad (14)$$

where the discrete definition of the total variation is expressed as

$$\text{TV}(u^n) = \sum_{-\infty}^{\infty} |u_{i+1}^n - u_i^n| \quad (15)$$

The sufficient conditions leading to an implicit TVD scheme is that  $\tilde{C}_{j\pm 1/2}$  and  $C_{j\pm 1/2}$  in Equation (10) should satisfy [18]

$$\tilde{C}_{j+1/2} \geq 0, \quad \tilde{C}_{j-1/2} \geq 0 \quad (16)$$

$$C_{j+1/2} \geq 0, \quad C_{j-1/2} \geq 0, \quad C_{j+1/2} + C_{j-1/2} \leq 1 \quad (17)$$

Subject to (16)–(17), free parameters chosen to obtain a TVD solution are as follows:

$$-\frac{1}{3} - \frac{(1 - \alpha - \omega + \gamma/2)v}{(1 - \omega)} - \frac{\gamma v^2}{(1 - \omega)} \geq 0 \tag{18a}$$

$$-\frac{1}{3} - \frac{(-1 + \alpha + \omega - \gamma/2)v}{(1 - \omega)} - \frac{\gamma v^2}{(1 - \omega)} \geq 0 \tag{18b}$$

$$\frac{1}{6} + \frac{(-\alpha + \gamma/2)v}{2(1 - \omega)} + \frac{(\frac{1}{2} + \omega/2 - \beta)v^2}{1 - \omega} \geq 0 \tag{18c}$$

$$\frac{1}{6} + \frac{(\alpha - \gamma/2)v}{2(1 - \omega)} + \frac{(\frac{1}{2} + \omega/2 - \beta)v^2}{1 - \omega} \geq 0 \tag{18d}$$

$$\frac{1 - \omega + 3v^2(\omega - 2\beta)}{3(1 - \omega)} \leq 1 \tag{18e}$$

For purposes of completeness, we plot in Figures 1(a) and 1(b) the TVD-satisfying range in the shaded areas at two arbitrarily chosen Courant numbers.

The explicit TG finite-element equation can be derived by enforcing  $\tilde{C}_{j+1/2} = \tilde{C}_{j-1/2} = 0$ . Depending on the Courant number  $v$ ,  $\alpha$  falling into the following equations should be chosen if the TVD solution is sought:

$$\frac{-\alpha(2 + 6v) + (1 - 6v^2)(1 - \omega - \gamma)}{\alpha} \geq 0 \tag{19a}$$

$$\frac{-\alpha(2 - 6v) + (1 - 6v^2)(1 - \omega - \gamma)}{\alpha} \geq 0 \tag{19b}$$

$$\frac{-(2\alpha + (1 - 6v^2)(1 - \omega - \gamma))}{6\alpha} \leq 1 \tag{19c}$$

Thus, the TVD-region is found in the range of

$$0 \leq \frac{-(2\alpha + (1 - 6v^2)(1 - \omega - \gamma))}{6\alpha} \leq 1 \tag{20}$$

The above TG finite-element model, while making the discrete model unconditionally monotonic, may simultaneously add artificial viscosity and make the discrete model overly diffusive in the sense that  $\gamma + \mu + \omega$  can by no means be equal to one. Therefore, it is impossible to obtain very accurate solutions using the proposed TVD finite-element model.

#### 4.2. M-matrix model

Another way of obtaining a monotonic solution for Equation (1) is to apply the  $M$ -matrix theory [19, 20]. For descriptive purposes, we can rewrite Equation (9) as

$$\underline{\underline{\mathbf{M}}}_c \mathbf{u}^{n+1} = \underline{\underline{\mathbf{C}}}\mathbf{f} + \underline{\underline{\mathbf{M}}}_c \mathbf{u}^n \tag{21}$$

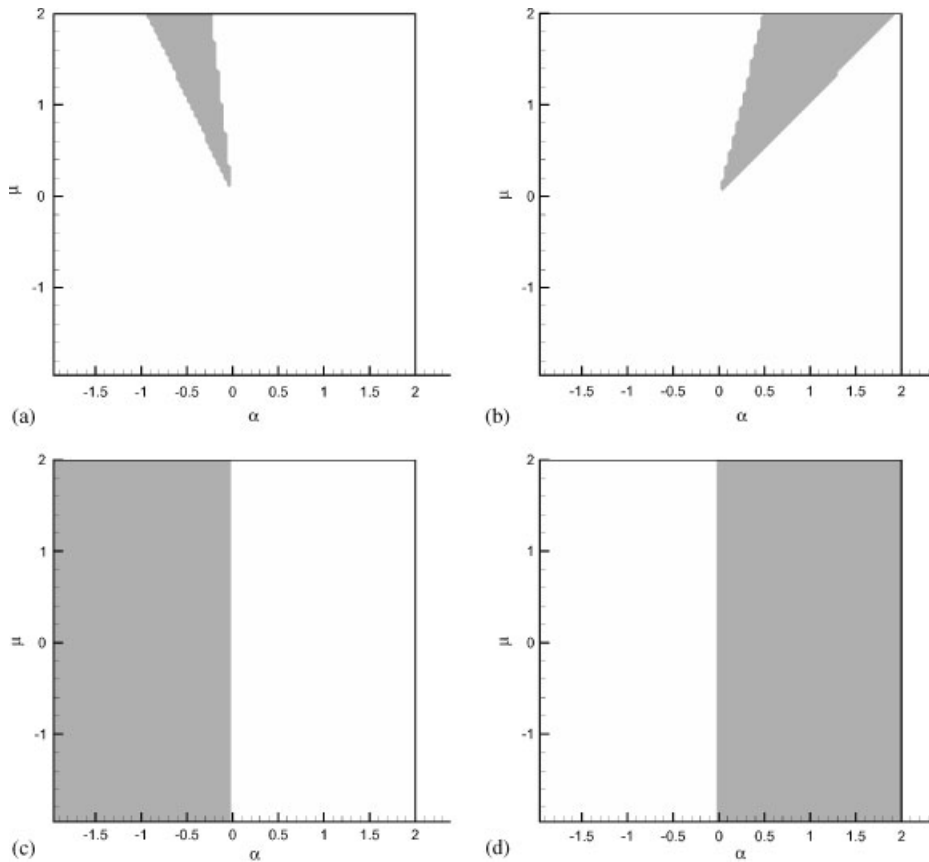


Figure 1. The shaded area of free parameters  $\alpha$  and  $\mu$  that satisfy the TVD and  $M$ -matrix conditions for the proposed consistent-mass TG finite-element model at different  $\nu$ : (a) Region that satisfies TVD condition at  $\nu=0.1$ , (b) region that satisfies TVD condition at  $\nu=0.7$ , (c) region that satisfies  $M$ -matrix condition at  $\nu=0.1$ , (d) region that satisfies  $M$ -matrix condition at  $\nu=0.7$ .

According to Ahués and Telias [20], the key to obtaining a monotone solution from a system of algebraic equations is that  $\underline{\mathbf{M}}_c$  ( $\equiv \underline{\mathbf{M}}_c - \underline{\mathbf{I}}$ , where  $\underline{\mathbf{M}}_c$  and  $\underline{\mathbf{I}}$  are known as the consistent mass and identity matrix, respectively) and  $\underline{\mathbf{C}}$  shown in (21) must be of  $M$ -matrix type. By definition, a matrix  $\underline{\mathbf{M}}_c$  is said to be an  $M$ -matrix if the following conditions hold:

- (i)  $\underline{\mathbf{M}}_c$  is an  $L$ -matrix, which implies  $\text{diag}(\underline{\mathbf{M}}_c) \geq 0$  and  $\text{diag}(\underline{\mathbf{M}}_c) - \underline{\mathbf{M}}_c \geq 0$ .
- (ii) There exists a diagonal matrix  $\underline{\mathbf{D}}$  ( $\equiv \text{diag}(d_{ij})$ ) such that  $\underline{\mathbf{D}} \underline{\mathbf{M}}_c$  is columnwise strictly diagonal dominant ( $\sum_i a_{ij} d_j > 0$ ), or that  $\underline{\mathbf{A}} \underline{\mathbf{D}}$  is rowwise strictly diagonal dominant ( $\sum_j a_{ij} d_j > 0$ ).

The above theorem guides our selection of free parameters to obtain a monotone solution from the discrete equation. Given a Courant number  $\nu$ , the range of validity for  $\alpha$ ,  $\beta$ ,  $\gamma$ , and

$\omega$  is determined from the following equations:

$$\frac{1-\omega}{3} + \left(1 - \alpha - \omega + \frac{\gamma}{2}\right)v + \gamma v^2 \geq 0 \quad (22a)$$

$$\frac{2(1-\omega)}{3} - \gamma v^2 \leq 0 \quad (22b)$$

$$\frac{1-\omega}{3} + \left(-1 + \alpha + \omega - \frac{\gamma}{2}\right)v + \gamma v^2 \geq 0 \quad (22c)$$

The  $M$ -matrix-satisfying regions are plotted in the shaded areas of Figures 1(c) and 1(d). As expected, the TVD region in Figures 1(a) and 1(b) falls entirely within the  $M$ -matrix region. We can, therefore, say that the shaded areas schematic in Figures 1(c) and 1(d) are  $M$ -matrix and TVD satisfying regions.

## 5. HIGH-ORDER SOLUTIONS

According to modified equation (12) for the investigated model equation, enforcement of  $\alpha + \beta = 1$ ,  $\gamma + \mu + \omega = 1$ ,  $\gamma = 2\alpha/7$  and  $\omega = \frac{1}{7}(7 - 12\alpha)$  can eliminate three leading discretization error terms. Considering  $\beta = 1 - \alpha$ ,  $\omega = \frac{1}{7}(7 - 12\alpha)$ ,  $\gamma = 2\alpha/7$  and  $\alpha = 7\mu/10$  in the high-order TG finite-element model, we need only to specify  $\alpha$  to close the model development. Our strategy of assigning value of  $\alpha$  is to make the high-order TG model less dispersive. Two theoretically rigorous theories, known as the group velocity theory and entropy increasing principle, are employed.

Subject to the initial condition  $u(x, t = 0) = \exp(ikx)$ , we can substitute (4) for  $u(x_j, t)$  into the finite-element equation (9). After some algebra,  $k_i$  and  $k_r$  can be derived in terms of  $\bar{\alpha}$  and  $v$  as follows:

$$k_i = -v^{-1} \tan^{-1}(C_1) \quad (23)$$

$$k_r = -v^{-1} \log(D_1 + D_2) \quad (24)$$

In the above,  $C_1$  and  $D_i$  ( $i = 1, 2$ ) are expressed as

$$C_1 = \frac{e_1}{e_2} \quad (25a)$$

$$D_1 = \frac{f_1}{f_2} \quad (25b)$$

$$D_2 = \frac{g_1}{g_2} \quad (25c)$$

where

$$\begin{aligned}
 e_1 &= 3v(4 - v^2 + (2 + v^2)\cos(\bar{\alpha}))(\cos(\bar{\alpha}) + \sin(\bar{\alpha})) \\
 e_2 &= (-4 + v^2)^2 + (2 + v^2)^2 \cos(\bar{\alpha})^2 + \cos(\bar{\alpha})(16 + 4v^2 - 2v^4 - 9v^2 \sin(\bar{\alpha})) \\
 f_1 &= 9v^2(4 - v^2 + (2 + v^2)\cos(\bar{\alpha}))^2(\cos(\bar{\alpha}) + \sin(\bar{\alpha}))^2 \\
 f_2 &= ((-4 + v^2)^2 + (16 + 4v^2 - 2v^4)\cos(\bar{\alpha}) + (4 + 13v^2 + v^4)\cos(\bar{\alpha})^2)^2 \\
 g_1 &= ((-4 + v^2)^2 + (2 + v^2)^2 \cos(\bar{\alpha})^2 + \cos(\bar{\alpha})(16 + 4v^2 - 2v^4 - 9v^2 \sin(\bar{\alpha})))^2 \\
 g_2 &= ((-4 + v^2)^2 + (16 + 4v^2 - 2v^4)\cos(\bar{\alpha}) + (4 + 13v^2 + v^4)\cos(\bar{\alpha})^2)^2
 \end{aligned}$$

### 5.1. Entropy-increasing finite-element model

Recall that the modified equation for the model equation has been derived as

$$\frac{\partial u}{\partial t} + c \frac{\partial u}{\partial x} = \sum_{n=2}^{\infty} \tau_n \frac{\partial^n u}{\partial x^n} \quad (26)$$

where  $\tau_n$  is the coefficient of the  $n$ th derivative term. Under the conditions  $\beta = 1 - \alpha$ ,  $\gamma = \frac{1}{3}$  and  $\omega = 1 - 3\alpha/2 - 3\gamma/4$ , which are used to eliminate the first two discretization error terms shown in Equation (12), the resulting four leading coefficients in the modified equation are expressed by

$$\tau_4 = \frac{\Delta x^4 v^2 (-1 + v^2)(-7 + 6\alpha)}{72 \Delta t (1 + 6\alpha)} \quad (27a)$$

$$\begin{aligned}
 \tau_5 &= \frac{1}{540(1 + 6\alpha)^2 \Delta t} (\Delta x^5 v (-1 + v^2) \\
 &\quad (-3 + 62v^2 + 36\alpha^2(-3 + 2v^2) - 12\alpha(3 + 8v^2))) \quad (27b)
 \end{aligned}$$

$$\begin{aligned}
 \tau_6 &= \frac{(-7 + 6\alpha)\Delta x^6 v^2 (-1 + v^2)}{1296(1 + 6\alpha)^3 \Delta t} \\
 &\quad (-3 + 26v^2 + 36\alpha^2(-3 + 2v^2) - 12\alpha(3 + 2v^2)) \quad (27c)
 \end{aligned}$$

Subject to the initial condition given in Section 2, the exact solution to the modified equation (26) can be derived as

$$u(x, t) = e^{pt} e^{ik(x-qt)} \quad (28)$$

where

$$p = \sum_{m=1}^{\infty} \tau_{2m} (-1)^m k^{2m} \quad (29a)$$

$$q = c - \sum_{m=1}^{\infty} \tau_{2m+1} (-1)^m k^{2m} \quad (29b)$$

Equations (28) and (2) reveal incorrect amplitude and propagation speed arising from the TG finite-element approximation. The task now is to control  $\alpha$  so as to minimize the erroneous wave propagation speed and prevent continuous growth of the amplitude error. In this study, we exploit the entropy-increasing principle [21] to achieve this goal.

Fulfillment of the theoretically plausible entropy-increasing principle requires that  $q_L > c > q_R$ , where  $q_L = (dx/dt)_L$  and  $q_R = (dx/dt)_R$ . On the left side of the discontinuity,  $q_L - c > 0$ , thus enabling us to obtain the following inequality relation:

$$\sum_{m=1}^{\infty} \tau_{2m+1} (-1)^m k^{2m} < 0 \quad (30)$$

As the mesh size  $\Delta x$  approaches zero,  $\tau_m (\equiv k_m (\Delta x)^{m-1})$  becomes negligibly small at larger  $m$ . Therefore, we can neglect the higher-order terms, shown in Equation (30), to obtain the following approximated expression:

$$(-1)^m \tau_{2m+1} < 0 \quad (31)$$

On the right side of the discontinuity, one can obtain a less dispersive solution using the same idea as that applied at the left side. Enforcing  $q_R - c < 0$ , we demand satisfaction of the following equation on the right side of the discontinuity:

$$\sum_{m=1}^{\infty} \tau_{2m+1} (-1)^m k^{2m} > 0 \quad (32)$$

As  $\Delta x$  approaches zero, the higher-order terms shown in Equation (32) can be omitted. For this reason, it suffices to apply the following approximated equation for a better agreement of the entropy-increasing principle:

$$(-1)^m \tau_{2m+1} > 0 \quad (33)$$

Provided that discontinuities appear, constraint conditions (31) and (33) are employed to minimize the dispersion error. The reduction of errors is particularly pronounced at high-frequency components.

Any improper specification of  $\alpha$  can cause the scheme to be anti-dissipative. Therefore,  $e^{p^t} < 1$  is enforced for making the TG model dissipative. That is,

$$\sum_{m=1}^{\infty} \tau_{2m} (-1)^m k^{2m} < 0 \quad (34)$$

Consider only the leading term shown in Equation (34), we then have

$$\tau_{2m} (-1)^m < 0 \quad (35)$$

Solutions which increase in magnitude with time are, thus, not permitted.

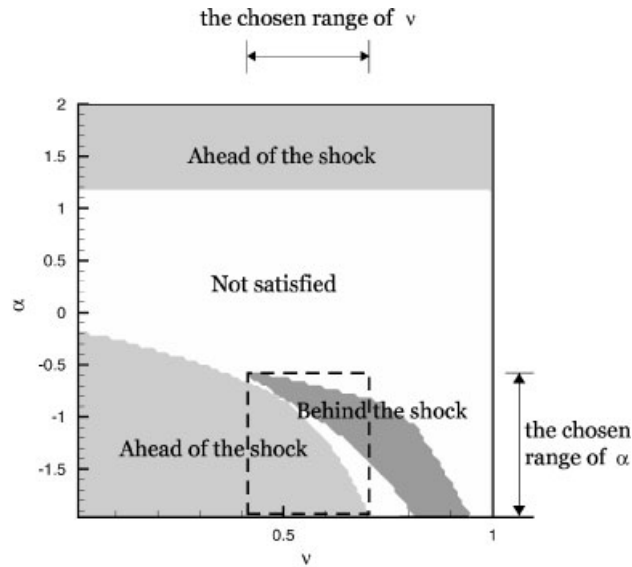


Figure 2. The range of  $\alpha$  against the Courant number  $v$  that satisfies the entropy-increasing principle (Up to the coefficient of  $u_{xxxxxxx}$  in the modified equation). The dashed box is the chosen entropy-increasing-satisfying region.

Through the above entropy-increasing principle, choice of  $\alpha$  is constrained by the following two equations for simultaneously satisfying equations (31), (33) and (35):

$$\text{ahead of the discontinuity } \tau_4 < 0, \tau_5 > 0, \tau_6 > 0, \tau_7 < 0 \tag{36}$$

$$\text{behind the discontinuity } \tau_4 < 0, \tau_5 < 0, \tau_6 > 0, \tau_7 > 0 \tag{37}$$

The stability regions ahead of and behind the discontinuity are shown in Figure 2. For the sake of completeness, the range of  $(\alpha, v)$  that is suitable for choice in the subsequent calculation is also schematic in the same figure.

### 5.2. Finite-element model based on the group velocity theory

As the modified equation (12) shows, use of TG model makes the modified equation dissipative and dispersive. The introduced dissipation error causes frequency-dependent attenuation of the Fourier components to occur; while the dispersion error results in erroneous wave number-dependent phase velocity. Therefore, it is necessary to derive the dispersion relation for the TG equation (9).

Our derivation starts with substitution of the analytic solution (2) into Equation (9). After cancelling out common factors, the dispersion equation for the proposed finite-element

equation is obtained as

$$\tan(\omega\Delta t) = \frac{\cos(\bar{\alpha})\sin(\bar{\alpha})A_1 + \sin(\bar{\alpha})A_2}{\cos(\bar{\alpha})^2A_3 + \cos(\bar{\alpha})A_4 + A_5 + \sin(\bar{\alpha})^2A_6} \quad (38)$$

Note that the analytic dispersion equation is  $\tan(\omega\Delta t) = \tan(v\bar{\alpha})$ . Coefficients shown in Equation (38) are as follows:

$$A_1 = \frac{-v}{9} (3 + (1 + 6\gamma - 18\gamma^2)v^2 + \omega^2(3 + v^2) - 2\omega(3 + (1 + 3\gamma)v^2)) \quad (39a)$$

$$A_2 = \frac{v}{9} (-6 + (1 + 6\gamma - 18\gamma^2)v^2 + \omega^2(-6 + v^2) - 2\omega(-6 + (1 + 3\gamma)v^2)) \quad (39b)$$

$$A_3 = \frac{(-1 + \omega - 3\gamma v^2)(-1 + (-1 + 3\gamma)v^2 + \omega(1 + v^2))}{9} \quad (39c)$$

$$A_4 = \frac{1}{9} (4 + v^2 + 6\gamma(-1 + 3\gamma)v^4 + \omega^2(4 + v^2) + 2\omega(-4 - v^2 + 3\gamma v^4)) \quad (39d)$$

$$A_5 = \frac{-((-2 + 2\omega + 3\gamma v^2)(2 + (-1 + 3\gamma)v^2 + \omega(-2 + v^2)))}{9} \quad (39e)$$

$$A_6 = \frac{-((-1 + \omega - 3\gamma)(-2 + 2\omega + 3\gamma)v^2)}{9} \quad (39f)$$

The energy spectrum over a length of  $2\Delta k$ , centred at  $k_0$ , transmits at a speed of  $C_g(\omega)$  ( $\equiv d\omega/dk|_{k_0}$ ) [10]. By definition, the group velocity for the proposed TG model can be derived by differentiating the dispersion equation, given in Equation (38), with respect to the wave number. The result is

$$D = \frac{C_g(\bar{\alpha}, v)}{c} = - \left( \frac{\mathbf{B}_1 + \mathbf{B}_2}{\mathbf{B}_3} \right) \quad (40)$$

In the above,

$$\mathbf{B}_1 = \frac{\mathbf{B}_{1a} \cdot \mathbf{B}_{1b}}{\mathbf{B}_{1c}} \quad (41a)$$

$$\mathbf{B}_2 = \frac{A_2 \cos(\bar{\alpha}) + A_1 \cos(\bar{\alpha})^2 - A_1 \sin(\bar{\alpha})^2}{A_5 + A_4 \cos(\bar{\alpha}) + A_3 \cos(\bar{\alpha})^2 + A_6 \sin(\bar{\alpha})^2} \quad (41b)$$

$$\mathbf{B}_3 = v \left( 1 + \frac{(A_2 \sin(\bar{\alpha}) + A_1 \cos(\bar{\alpha}) \sin(\bar{\alpha}))^2}{(A_5 + A_4 \cos(\bar{\alpha}) + A_3 \cos(\bar{\alpha})^2 + A_6 \sin(\bar{\alpha})^2)^2} \right) \quad (41c)$$

$$\mathbf{B}_{1a} = -(A_2 \sin(\bar{\alpha}) + A_1 \cos(\bar{\alpha}) \sin(\bar{\alpha})) \quad (41d)$$

$$\mathbf{B}_{1b} = -(A_4 \sin(\bar{\alpha})) - 2A_3 \cos(\bar{\alpha}) \sin(\bar{\alpha}) + 2A_6 \cos(\bar{\alpha}) \sin(\bar{\alpha}) \quad (41e)$$

$$\mathbf{B}_{1c} = (A_5 + A_4 \cos(\bar{\alpha}) + A_3 \cos(\bar{\alpha})^2 + A_6 \sin(\bar{\alpha})^2)^2 \quad (41f)$$

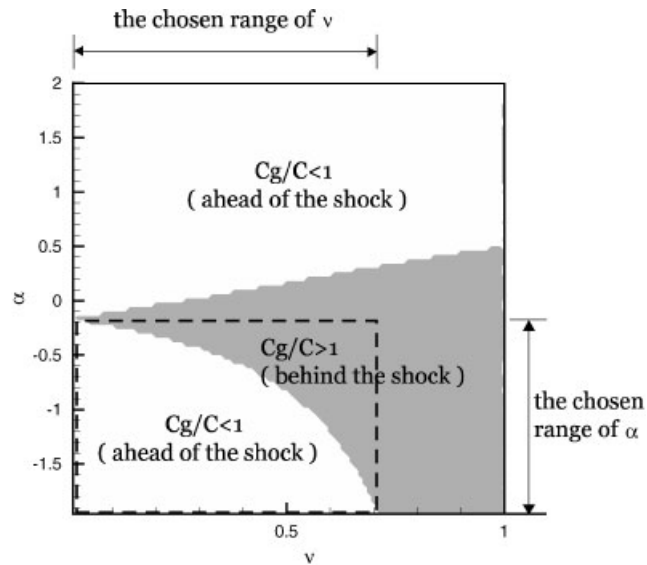


Figure 3. Plot of  $C_g/c$  against  $\alpha$  and  $v$  for the proposed TG model applied in regions ahead and behind of the discontinuity. The dashed box is the chosen group-velocity-theory-satisfying region.

By virtue of the above-derived group velocity, we can plot in Figure 3 regions with  $D > 1$  and  $D < 1$  against the modified wave number  $\bar{\alpha}$  at different values of  $\alpha$  and  $v$ . Given a value of  $v$ , this plot helps to determine  $\alpha$  mostly suited to yield the less dispersive solutions. Ahead of the discontinuity, the region with  $D < 1$  is chosen. In contrast, the region with  $D > 1$  is considered for parameters used behind the discontinuity. The range that can be chosen to obtain the group-velocity-theory-satisfying solution is also schematically given in Figure 3.

Taking Figures 2 and 3 into consideration, the  $(\alpha, v)$  regions that satisfy both entropy increasing and group velocity theories ahead and behind of discontinuities are plotted in Figures 4(a) and 4(b), respectively. The region of  $\alpha$ , which is a function of  $v$ , that can be chosen to obtain the theoretically rigorous less dispersive solution is given in Figure 5. Two sets of  $(\alpha, v)$  at points marked by 'X' in the figure are used in the regions ahead of and behind the discontinuity, respectively.

The  $\alpha$  thus far determined is subject to an additional constraint for obtaining an even better solution. For stability reasons, it is required that  $k_r > 0$  for making the TG model dissipative. For this reason, we plot  $k_r$  against  $\bar{\alpha}$  in Figure 6, from which it is demonstrated that  $k_r > 0$  for all  $\alpha$ . In the whole wave-number spectrum, the computed non-constant group velocities explain why oscillations are seen in the numerical solution. It is, thus, important to judiciously select  $\alpha$  so as to control the phase velocity and, thus, avoid non-physical oscillations. Figure 7, which plots the  $k_i$  against the modified wave number  $\bar{\alpha}$ , reveals that  $\partial k_i / \partial \bar{\alpha}$  is fairly close to one in the vicinity of  $\bar{\alpha} = 0$ , implying that  $k_i$  approaches  $\bar{\alpha}$  in the small wave-number range no matter what the Courant number is. While  $k_i$  increasingly deviates from  $\bar{\alpha}$  at a very large wave number, the Fourier coefficients in the Euler formula [22] asymptotically approach zero. Under the circumstances, large wave number are, fortunately, of no significant contribution to the evolving solution. As Figure 7 reveals, the erroneous dispersive nature of

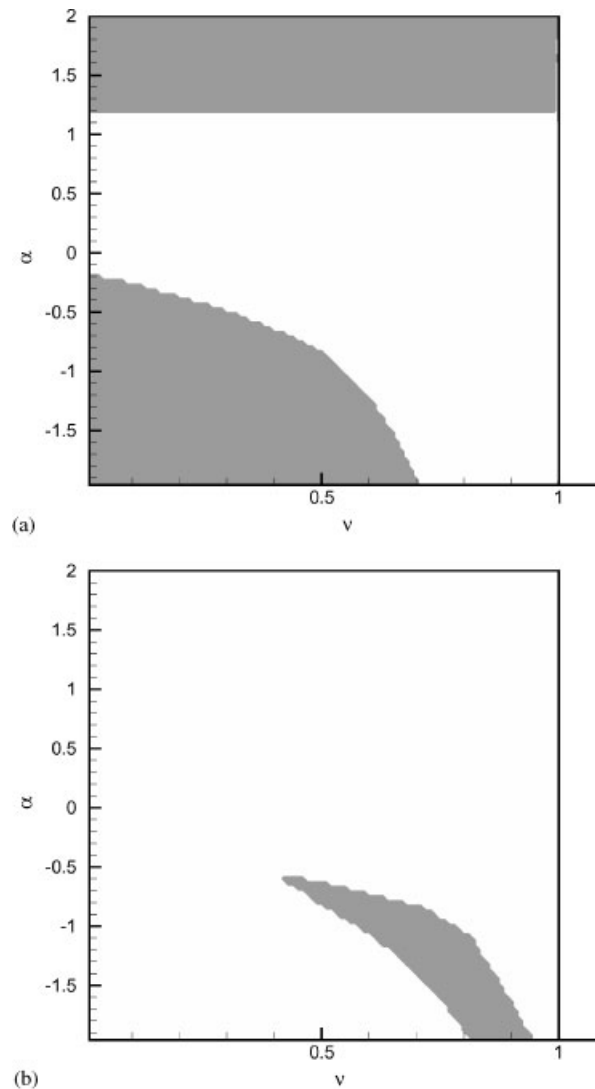


Figure 4. The range of  $\alpha$  against the Courant number  $v$  that satisfies both the entropy-increasing principle and group velocity theory: (a) Ahead of the shock, the shaded areas satisfy the entropy-increasing and group velocity theories, (b) behind the shock, the shaded area satisfies the entropy-increasing and group velocity theories.

solution in regions immediately behind the shock warrants a care owing to its less accurate representation.

The coefficients for the Fourier components with a large wave number are large in magnitude. Any dispersive error can cause the solution to deteriorate considerably. In the small wave-number case,  $u$  can quickly disperse into a train of oscillations at the back of the wave. The higher the wave number, the severer the oscillation since  $k_i$ , as shown in Equation (23),

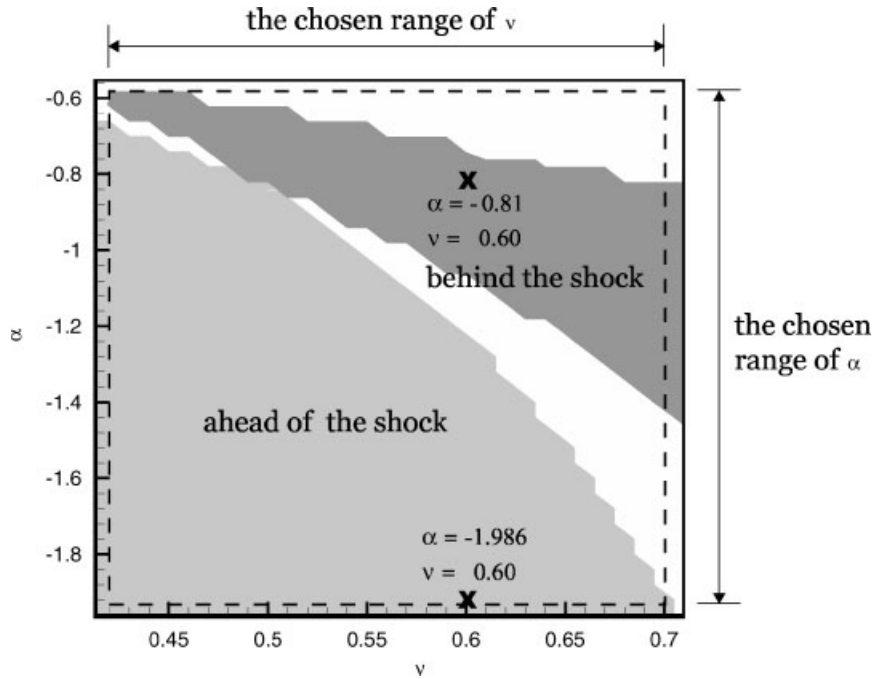


Figure 5. The shaded area is the region for obtaining solutions that satisfy the entropy-increasing and group velocity theories.

deviates from its exact value in the direction of increasing wave number. Such oscillatory solutions are due mainly to phase lagging if the Fourier component for a high wave number is not negligibly small. When specifying free parameters which can render  $dk_i/d\bar{\alpha} < 1$ , it is expected to see a train of oscillations behind the pulse [11]. Therefore, free parameters are sought to yield  $\partial k_i/\partial \bar{\alpha} > 1$ , thus preventing oscillations from occurring behind a pulse wave. In contrast to oscillations found behind the pulse wave, the oscillations ahead of the pulse are the direct result of a faster numerical group velocity [11]. The cure for this upstream oscillation being the avoidance of  $\partial k_i/\partial \bar{\alpha} > 1$ . Therefore, it is imperative that  $dk_i/d\bar{\alpha} < 1$  in front of the pulse while  $dk_i/d\bar{\alpha} > 1$  behind the pulse for controlling high-frequency (or high wave number) oscillations in the vicinity of high gradient solutions. The fact that  $\partial^2 u/\partial x^2 \partial u/\partial x < 0$  ahead of the shock and  $\partial^2 u/\partial x^2 \partial u/\partial x > 0$  behind the shock [1] provides us impetus to suppress much of the high-frequency oscillation found in the vicinity of discontinuity by enforcing

$$\frac{dk_i}{d\bar{\alpha}} > 1 \quad \text{if } SS(u) > 0 \tag{42}$$

$$\frac{dk_i}{d\bar{\alpha}} < 1 \quad \text{if } SS(u) < 0 \tag{43}$$

In the above, the shock structure function  $SS(u) (\equiv \text{sign}(\partial^2 u/\partial x^2 \partial u/\partial x))$  is adopted. As for the smooth flow case where  $|SS(u)| < \epsilon$  (Here,  $\epsilon$  is a small positive number), we choose free parameters that can render a solution of high-order accuracy.

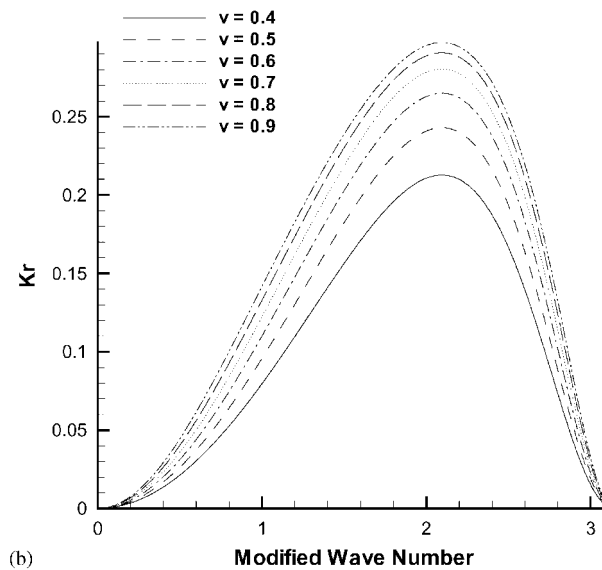
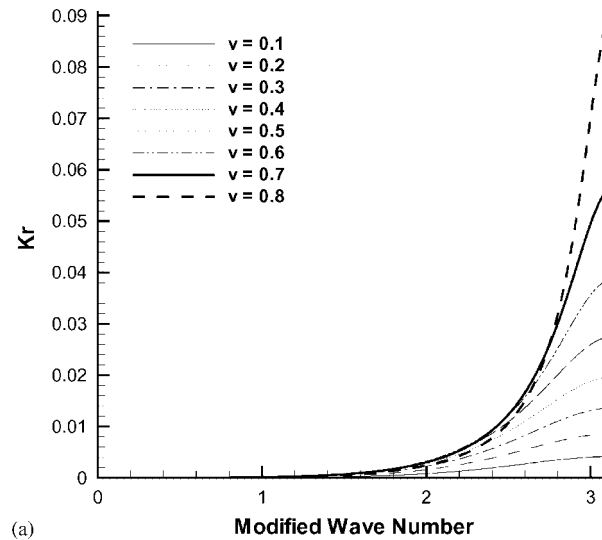
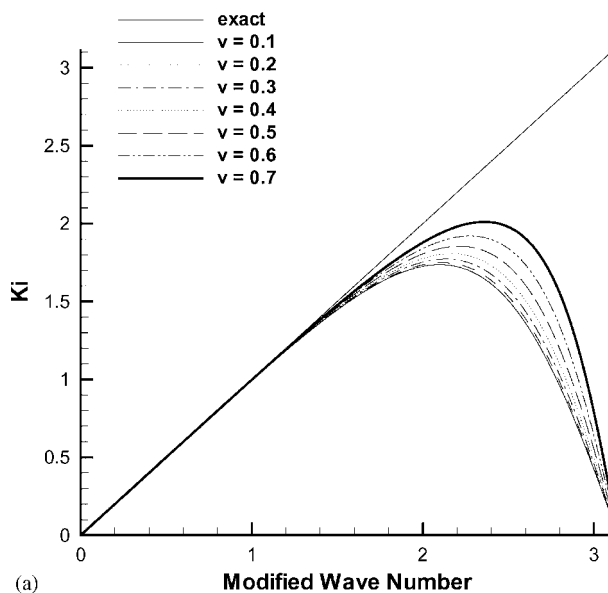


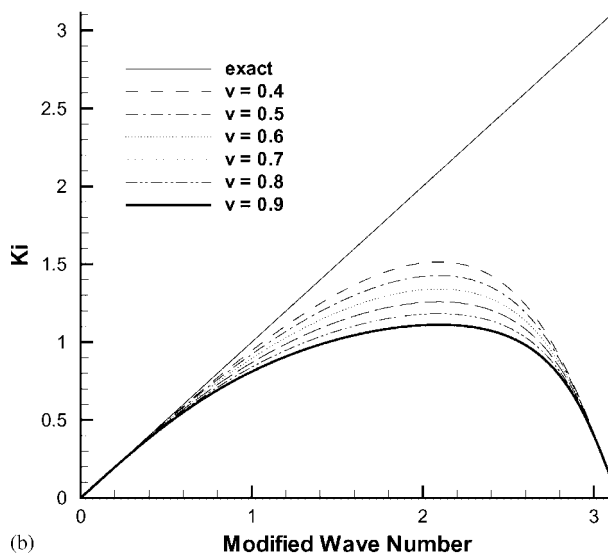
Figure 6. Plot of  $K_r$  against the modified wave number for the proposed TG model at different Courant numbers  $\nu$ : (a) Plot of  $K_r$  against the modified wave number for the TG model applied ahead of the discontinuity, (b) plot of  $K_r$  against the modified wave number for the proposed TG model applied behind the discontinuity.

## 6. COMPUTED RESULTS

Based on the theories summarized in Figures 1 and 5, all results presented below were obtained at  $\nu=0.6$ . The reason is that all free parameters can be rigorously chosen to render



(a)



(b)

Figure 7. Plot of  $K_i$  against the modified wave number for the proposed TG model at different Courant numbers  $v$ : (a) Plot of  $K_i$  against the modified wave number for the proposed TG model applied ahead of the discontinuity, (b) plot of  $K_i$  against the modified wave number for the proposed TG model applied behind the discontinuity.

both monotonic and high-order solutions (refer to Figures 5 and 8). In Table I, we tabulate the chosen parameters for the monotonic TG model. In addition, parameters used in the high-order model in regions ahead of and behind the discontinuity are all tabulated in the same table.

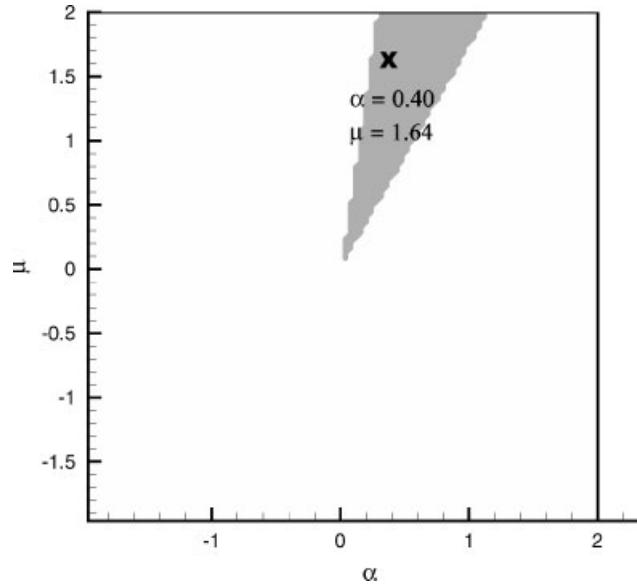


Figure 8. The shaded area is the TVD and  $M$ -matrix satisfying region. The values at  $X$  are used in the monotonic finite-element model.

Table I. Parameters used in the calculations.

| Free parameter | Monotonic model | Less dispersive high-order model ahead of the discontinuity | Less dispersive high-order model behind the discontinuity |
|----------------|-----------------|---|---|
| $\alpha$       | 0.4             | -1.986  | -0.81   |
| $\beta$        | 0.6             | 2.986   | 1.81  |
| $\gamma$       | -0.6896         | 0.3333  | 0.3333  |
| $\mu$          | 1.84            | -3.0683   | -1.29833  |
| $\omega$       | 0.2551          | 3.729   | 1.965   |

As a first step towards verifying the proposed finite-element model, we considered a pure advection equation in the specified flow. The problem defined in  $-1 \leq x \leq 1$  involves smooth as well as discontinuous profiles

$$u(x, 0) = \begin{cases} 0.5\sqrt{1 - 100(x - 0.2)^2}; & 0.1 < x \leq 0.3 \\ 0.5; & 0.4 < x \leq 0.6 \\ 0.25[\cos(\frac{(x-0.8)\pi}{0.1}) + 1]; & 0.7 < x \leq 0.9 \\ 0; & \text{otherwise} \end{cases} \quad (44)$$

Given a mesh size of  $\Delta x = 0.01$ , the time increment was chosen to be  $\Delta t = 0.01$ . This test serves to demonstrate that the FCT TG model can resolve discontinuities.

We will show a comparison of TG finite-element solutions with the exact solution. It is evident from Figure 9 that the solutions, which are obtained from the finite-element models

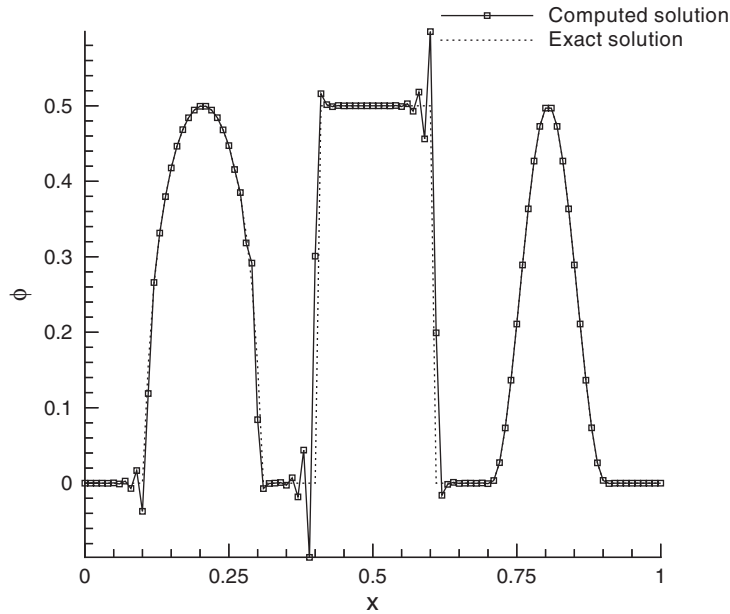


Figure 9. The computed entropy-increasing finite-element solution (symbol) that satisfies the entropy increasing and group velocity theories and the exact solution (dotted).

derived using the entropy-increasing principle and the group velocity theory, are in good agreement with the exact solution, except in regions near the jump. Figure 10 shows the low-order solutions, which are obtained in a sense that both TVD and  $M$ -matrix conditions are satisfied. As a result, solutions are all shown to be oscillation free. Having obtained the accurate but dispersive solution and the unconditionally monotonic solution, we can apply them in combination by virtue of the flux corrected transport technique of Boris and Book [23]. Numerical evidence, as shown in Figure 11, clearly shows that solutions obtained at  $t = 1$  were accurately predicted without observed oscillations.

The second test involved a propagating piecewise continuous profile in the following non-linear system:

$$u_t + uu_x = 0 \quad (45)$$

Subject to the initial condition given by

$$u(x, 0) = \begin{cases} 1; & x \leq 1.5 \\ 2.5 - x; & 1.5 < x \leq 2.5 \\ 0 & x > 2.5 \end{cases} \quad (46)$$

the exact solution in  $0 \leq x \leq 4$  takes the following form [24]:

$$u(x, t < 1) = \begin{cases} 1; & x \leq 1.5 + t \\ \frac{2.5-x}{1-t}; & 1.5 + t < x \leq 2.5 \\ 0; & x > 2.5 \end{cases} \quad (47)$$

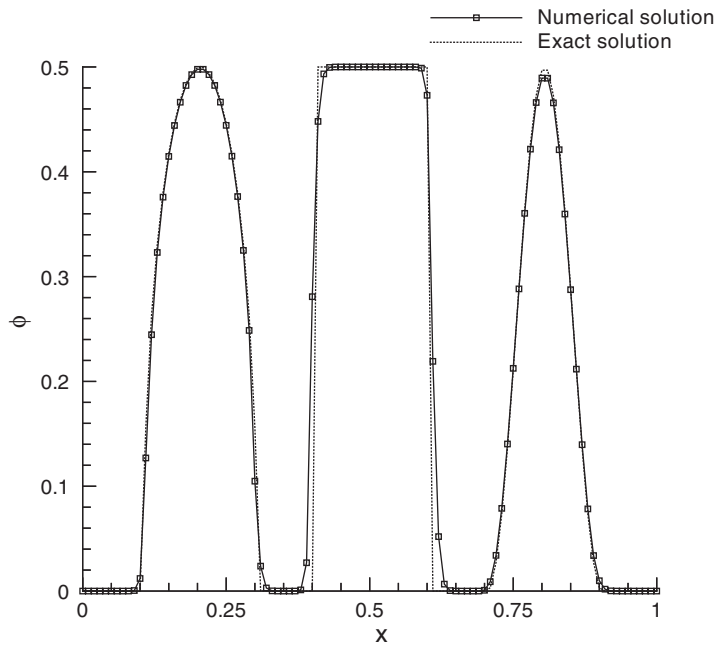


Figure 10. The computed  $M$ -matrix and TVD-satisfying finite-element solution (symbol) and exact solution (dotted), at  $t=0.05$  s under  $\nu=0.1$  and  $\Delta x = \Delta t = 0.01$ .

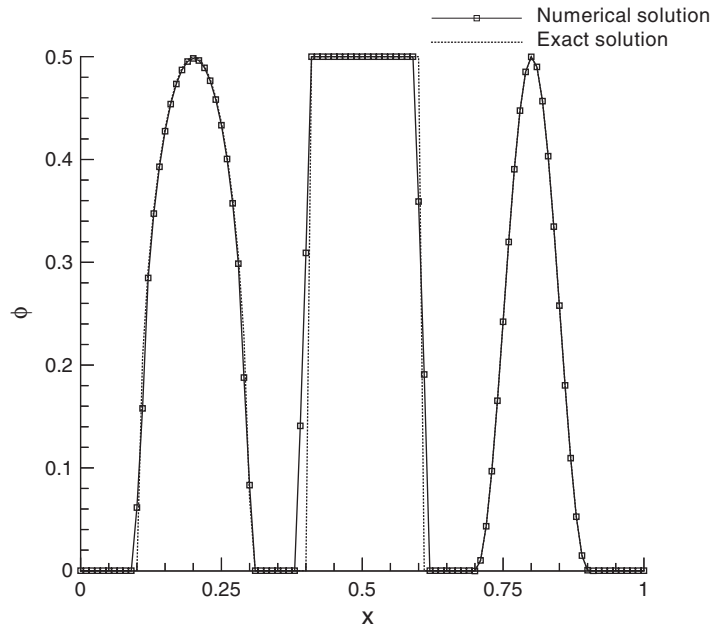


Figure 11. The computed FCT finite-element solution (symbol) and exact solution (dotted) at  $t=0.005$  s under  $\nu=0.1$  and  $\Delta x = \Delta t = 0.001$ .

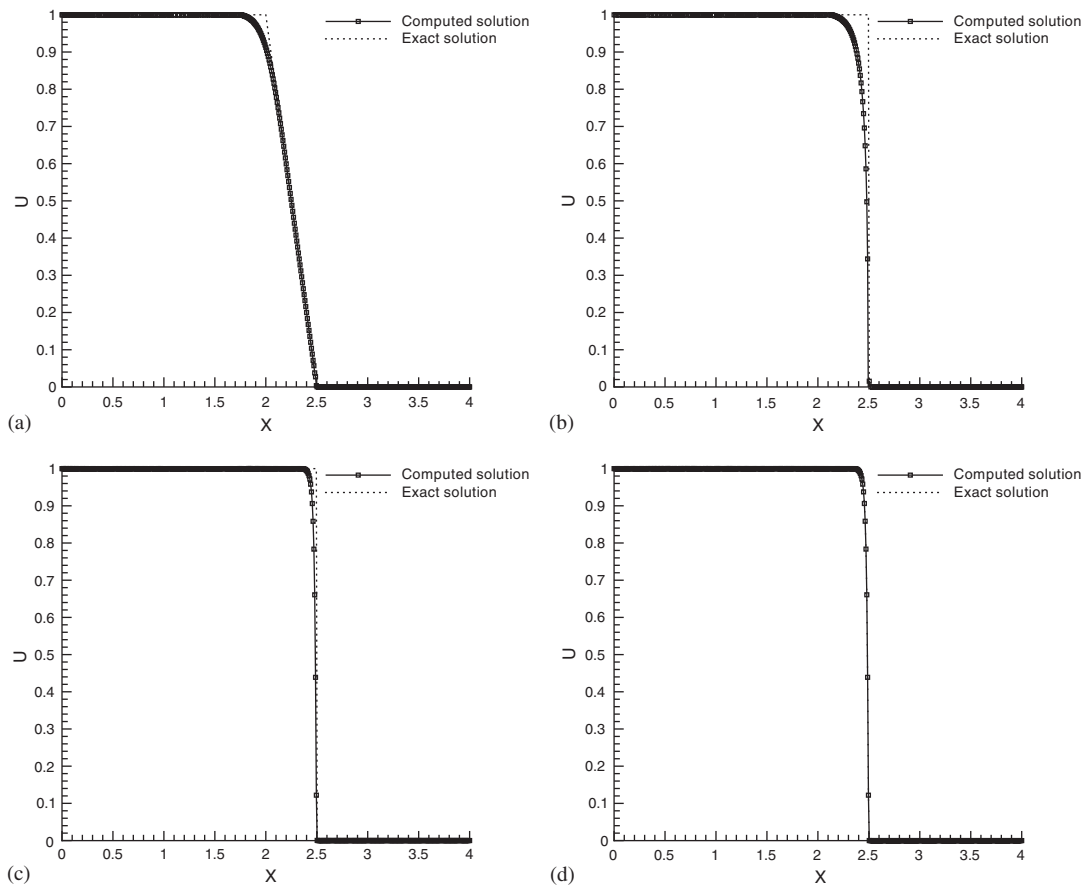


Figure 12. The computed FCT solutions for the non-linear problem at (a)  $t = 0.5$ , (b)  $t = 1$ , (c)  $t = 1.5$ , (d)  $t = 2$ .

or

$$u(x, t > 1) = \begin{cases} 1; & x \leq 2 + 0.5t \\ 0; & x > 2 + 0.5t \end{cases} \quad (48)$$

This problem is chosen since the non-linear term will evolve to show a discontinuity at  $x = 0.25$  when  $t = 1$ . Finite-element solutions, which were obtained at  $\Delta x = 0.04$  and  $0.005$  ( $\nu = 0.125$ ), are shown in Figure 12 at  $t = 0.5, 1, 1.5$  and  $2$ .

## 7. CONCLUDING REMARKS

This paper has presented a TG finite-element model for the first-order hyperbolic equation. Free parameters introduced into the model development have been theoretically determined to

obtain solutions in regions of sharp profiles using the theories of TVD and the  $M$ -matrix. The resulting TG finite-element models, while making the solutions unconditionally monotonic and, thus, stable, effectively add positive artificial viscosity to the non-dispersive hyperbolic model equation. To avoid making these models overly diffusive, high-order finite-element model, that is necessary to obtain the FCT solution, is also rigorously constructed. In the smooth flow, we employed the modified equation analysis to construct the high-order model. In the presence of discontinuities, we construct the dispersively more accurate finite-element model using the concept of group velocity. By theory, we demand that the group velocity of the discrete model be larger than the analytic phase velocity behind the shock. In contrast, the group velocity should be slower than the analytic phase velocity in front of the shock. Use of these two constraint conditions helps us to reduce errors of the high-frequency (or high wave number) type. Another guideline for developing the high-order TG model is the use of entropy-increasing principle. Guided by this principle, we can properly choose free parameters so as to render correct signs in the coefficients of the first five leading discretization error terms and, thus, eliminate much of the dispersive errors. Calculations have shown that all theoretically supported TG models are well performed.

#### APPENDIX A

According to Equation (28), we can easily express  $u$  as

$$u = e^{(p-ikq)t} e^{ikx} \quad (\text{A1})$$

This is followed by performing time and spatial derivatives on  $u$ , leading to

$$u_t = (p - ikq)u \quad (\text{A2})$$

$$u_x = iku \quad (\text{A3})$$

$$u_{xx} = (ik)^2 u = -k^2 u \quad (\text{A4})$$

$$u_{xxx} = (ik)^3 u = -ik^3 u \quad (\text{A5})$$

$$u_{xxxx} = (ik)^4 u = k^4 u \quad (\text{A6})$$

$$u_{xxxxx} = (ik)^5 u = ik^5 u \quad (\text{A7})$$

⋮

By substituting Equations (A2) and (A3) into (1), we have

$$\begin{aligned} u_t + cu_x &= (p - ikq + ick)u \\ &= [p + ik(c - q)]u \end{aligned} \quad (\text{A8})$$

According to Equations (29a) and (29b), we have

$$\begin{aligned} u_t + cu_x &= \left[ p + ik \sum_{m=1}^{\infty} \tau_{2m+1} (-1)^m k^{2m} \right] u \\ &= \left[ \sum_1^{\infty} \tau_{2m} (-1)^m k^{2m} + ik \sum_1^{\infty} \tau_{2m+1} (-1)^m k^{2m} \right] u \end{aligned} \quad (\text{A9})$$

or

$$\begin{aligned} u_t + cu_x &= -\tau_2 k^2 + \tau_4 k^4 - \tau_6 k^6 + \tau_8 k^8 + \dots \\ &\quad + ik[-\tau_3 k^2 + \tau_5 k^4 - \tau_7 k^6 + \tau_9 k^8 + \dots] \end{aligned} \quad (\text{A10})$$

By substituting (A4)–(A7) into  $\sum_{n=2}^{\infty} \tau_n \partial^n u / \partial x^n$ , we can have

$$\sum_{n=2}^{\infty} \tau_n \frac{\partial^n u}{\partial x^n} = (-k^2 \tau_2 - ik^3 \tau_3 + k^4 \tau_4 + ik^5 \tau_5 + \dots) u \quad (\text{A11})$$

Inspecting Equations (A10) and (A11), we can prove that Equation (28), together with equations (29a) and (29b), is the exact solution of (1).

#### ACKNOWLEDGEMENTS

This work was supported by the National Science Council of the Republic of China, NSC 88-2611-E-002-025.

#### REFERENCES

1. LeVeque RJ. *Numerical Methods for Conservation Laws* (2nd edn). Birkhäuser Verlag: Basel, 1992.
2. Morton KW. Generalized Galerkin methods for hyperbolic problems. *Computer Methods in Applied Mechanical Engineering* 1985; **52**:847–871.
3. Lesaint P, Raviart PA. On a finite-element method for solving the neutron transport problems. In *Mathematical Aspects of Finite Elements in Partial Differential Equations*, de Boor C (ed). Academic Press: New York, 1974; 89–123.
4. Lee JHW, Peraire J, Zienkiewicz OC. The characteristic Galerkin method for advection dominated problems—an assessment. *Computer Methods in Applied Mechanical Engineering* 1987; **61**:359–369.
5. Hughes TJR, Mallet M, Mizukami A. A new finite-element formulation for computational fluid dynamics: II. Beyond SUPG. *Computer Methods in Applied Mechanical Engineering* 1986; **54**:341–355.
6. Christie I, Griffiths DF, Mitchell AR, Zienkiewicz OC. Finite-element methods for second order differential equations with significant first derivatives. *International Journal for Numerical Methods in Engineering* 1976; **10**:1389–1396.
7. Donea J. A Taylor–Galerkin method for convective transport problems. *International Journal for Numerical Methods in Engineering* 1984; **20**:101–119.
8. Tworzydło WW, Oden JT, Thornton EA. Adaptive implicit/explicit finite-element method for compressible viscous flows. *Computer Methods in Applied Mechanical Engineering* 1992; **95**:397–440.
9. Safian A, Oden JT. High-order Taylor–Galerkin method for linear hyperbolic systems. *Journal of Computational Physics* 1995; **120**:206–230.
10. Trefethen LN. *Wave Propagation and Group Velocity*. Academic Press: New York, 1960.
11. Trefethen LN. Group velocity in finite difference scheme. *SIAM Review* 1982; **14**(2):113–136.
12. Cathers B, O’connor BA. The group velocity of some numerical schemes. *International Journal for Numerical Methods in Fluids* 1985; **5**:201–224.
13. Natter GF, Schneider GE. Use of the second law for artificial dissipation in compressible flow discrete analysis. *Journal of Thermophysics and Heat Transfer* 1994; **8**(3):500–506.

14. Lax PD. *Hyperbolic System of Conservation Laws and the Mathematical Theory of Shock Waves*. Society for Industrial and Applied Mathematics: Philadelphia, PA, 1972.
15. Baker AJ, Kim JW. A Taylor weak-statement algorithm for hyperbolic conservation laws. *International Journal for Numerical Methods in Engineering* 1987; **7**:489–520.
16. Warming RF, Hyett BJ. The modified equation approach to the stability and accuracy analysis of finite difference methods. *Journal of Computational Physics* 1974; **14**:159–179.
17. Lax PD. Weak solutions of nonlinear hyperbolic equations and their numerical computation. *Communications in Pure and Applied Mathematics* 1954; **2**:159–193.
18. Harten A. High resolution schemes for hyperbolic conservation laws. *Journal of Computational Physics* 1983; **49**:357–393.
19. Meis T, Marcowitz U. Numerical solution of partial differential equations. *Applied Mathematical Sciences*, vol. 32. Springer: New York, 1981.
20. Ahués M, Talias M. Petrov–Galerkin scheme for the steady state convection diffusion equation. *Finite Elements in Water Resources* 1982; **2**(3).
21. Zhang H, Lee Q, Zhuang F. On the construction of high order accuracy difference schemes. *ACTA Aerodynamica Sinica* 1998; **16**(1):14–23.
22. Kreyszig E. *Advanced Engineering Mathematics* (3rd edn). Wiley, Inc.: New York, 1972.
23. Boris JP, Book DL. Flux corrected transport, SHASTA, a fluid transport algorithm that works. *Journal of Computational Physics* 1973; **11**:38–69.
24. Shin BR, Ikohagi T, Daiguji H. A modified QUICK scheme with good stability and high convergence rate. *Computational Fluid Dynamics Journal* 1998; **7**(3):283–299.